ELSEVIER

Journal of Organometallic Chemistry 642 (2002) 227–236

Journal of Organometallic Chemistry

www.elsevier.com/locate/jorganchem

Phosphorus–hydrogen bond cleavage on a Ph_2PH-substituted μ_3-thioxo dicobalt–iron cluster as a route to bridging phosphido and thiophosphine ligands

Jason D. King [a], Martin J. Mays [a,*], Chi-Yu Mo [a], Gregory A. Solan [b], Gráinne Conole [c], Mary McPartlin [c]

[a] *University Chemical Laboratory, Department of Chemistry, Lensfield Road, Cambridge CB2 1EW, UK*
[b] *Department of Chemistry, University of Leicester, University Road, Leicester LE1 7RH, UK*
[c] *School of Applied Chemistry, University of North London, Holloway Road, London N7 8DB, UK*

Received 2 August 2001; accepted 21 August 2001

Abstract

The secondary phosphine-substituted (at cobalt) mixed-metal dicobalt–iron complex $[Co_2Fe(\mu_3\text{-}S)(CO)_8(PPh_2H)]$ (**1**) can be prepared in good yield from the reaction of $[Co_2Fe(\mu_3\text{-}S)(CO)_9]$ with one equivalent of Ph_2PH in toluene. Also isolated in the reaction, as minor products, are the disubstituted (both at cobalt) complex $[Co_2Fe(\mu_3\text{-}S)(CO)_7(PPh_2H)_2]$ (**2**) and the trisubstituted species $[Co_2Fe(\mu_3\text{-}S)(CO)_6(PPh_2H)_3]$ (**3**). Thermolysis of **1** or **2** results in P–H bond cleavage and the formation of the bis-phosphido-bridged species $[Co_2Fe(\mu_3\text{-}S)(\mu\text{-}PPh_2)_2(CO)_6]$ (**4**) and $[Co_2Fe(\mu_3\text{-}S)(\mu\text{-}PPh_2)_2(CO)_5(PPh_2H)]$ (**5**). Complex **5** can also be prepared more directly by treatment of **4** with one equivalent of Ph_2PH. The X-ray structure of the $PhPMe_2$ analogue of **5**, $[Co_2Fe(\mu_3\text{-}S)(\mu\text{-}PPh_2)_2(CO)_5(PPhMe_2)]$ (**5′**), reveals the phosphine to be cobalt-bound and occupying an equatorial site. Carbonylation of **4** results in coupling of one phosphido group with the sulphur cap to give the thiophosphine-bridged complex $[Co_2Fe(\mu_3\text{-}SPPh_2)(\mu\text{-}PPh_2)(CO)_7]$ (**6**), while treatment of **1** with *n*-BuLi followed by $RSCH_2Cl$ ($R = Me$, Ph) results in the formation of the previously reported thiophosphinomethane-bridged species $[Co_2Fe(\mu_3\text{-}S)(\mu\text{-}PPh_2CH_2SR)(CO)_8]$ ($R = Me$ **7a**, Ph **7b**). In contrast, interaction of **1** with *n*-BuLi followed by successive treatment with carbon disulphide and methyl iodide yields the dithiomethoxycarbonylphosphine-bridged complex $[Co_2Fe(\mu_3\text{-}S)\{\mu\text{-}PPh_2C(SMe){=}S\}(CO)_8]$ (**8**). Single crystal X-ray diffraction studies have been performed on complexes **5′** and **8**. © 2002 Elsevier Science B.V. All rights reserved.

Keywords: Cobalt; Iron; Phosphido; Thiophosphine; Thiophosphinomethane; Dithioalkoxycarbonylphosphine; Cluster

1. Introduction

The scission of a P–H bond of a secondary phosphine within the co-ordination sphere of a transition metal complex either thermolytically, photolytically or with a strong base has been the subject of numerous reports [1–5]. Thermolysis or photolysis can lead via oxidative addition to the formation of phosphide and hydride groups which, in the presence of more than one metal centre, can form complexes in which these ligands act as bridges [1,2]. Conversely, deprotonation of the phosphine followed by reaction of the resulting anion with a wide variety of electrophiles can be employed to furnish novel phosphine ligands, some of which are not obtainable by alternative routes [3–5].

Recently, we have been interested in multidentate unsymmetrical ligands containing phosphorus and sulphur donor atoms and have prepared bimetallic transition metal carbonyl complexes incorporating neutral and monoanionic ligands of the type, $Ph_2P(SR)$ [6], Ph_2PCH_2SR [7], $[Ph_2PS]^-$ [8], $[Ph_2PCH{=}CRS]^-$ [9] and $[Ph_2PCH{=}CRCPhC{=}S]^-$ [8] ($R = $ hydrocarbyl). Two synthetic approaches have, in general, been employed, namely reaction of the metal carbonyl complex with the pre-prepared ligand or generation of the ligand in situ on the bimetallic backbone.

---

* Corresponding author.
E-mail address: mjm14@cam.ac.uk (M.J. Mays).

PII: S0022-328X(01)01227-X

Herein we report our findings on the synthesis and characterisation of the secondary phosphine substituted dicobalt–iron cluster $[Co_2Fe(\mu_3\text{-}S)(CO)_8(PPh_2H)]$ **1** along with the results of our experiments on the thermolysis of **1**, and on its deprotonation and subsequent reaction with sulphur-containing electrophiles. Additionally, we report the reactions of $[Co_2Fe(\mu_3\text{-}S)(\mu\text{-}PPh_2)_2(CO)_6]$ **4** with CO and organophosphines.

2. Results and discussion

2.1. *Reaction of [$Co_2Fe(\mu_3$-S)(CO)$_9$] with Ph_2PH*

The reaction of $[Co_2Fe(\mu_3\text{-}S)(CO)_9]$ with one equivalent of Ph_2PH in toluene at 313 K gives the monosubstituted complex $[Co_2Fe(\mu_3\text{-}S)(CO)_8(PPh_2H)]$ **1** in 62% yield, the disubstituted derivative $[Co_2Fe(\mu_3\text{-}S)(CO)_7(PPh_2H)_2]$ **2** in 8% yield and the trisubstituted derivative $[Co_2Fe(\mu_3\text{-}S)(CO)_6(PPh_2H)_3]$ **3** (Scheme 1) in 4% yield. Complexes **1**–**3** have been characterised by mass spectrometry, microanalysis and by ^1H-, ^{31}P-, ^{13}C-NMR and IR spectroscopy (see Table 1 and Section 3).

The spectroscopic properties of **1**–**3** in solution are consistent with those found by Aime et al. in their studies of the products of carbonyl substitution by tertiary phosphines in $[Co_2Fe(\mu_3\text{-}S)(CO)_9]$ [10]. The spectroscopic data suggest that the Ph_2PH ligands in **1**–**3** occupy equatorial sites on one Co, two Co's, and two Co's and one Fe, respectively. Furthermore, a Mössbauer study of $[Co_2Fe(\mu_3\text{-}S)(CO)_8(PPh_3)]$ [11] indicates monosubstitution to occur at cobalt at an equatorial site and this is supported by the X-ray structure of the related triphenylphosphite complex $[Co_2Fe(\mu_3\text{-}S)(CO)_8\{P(OPh)_3\}]$ [12].

For **1**, the IR spectrum is similar to those reported for other monosubstituted phosphine derivatives of $[Co_2Fe(\mu_3\text{-}S)(CO)_9]$ [10], and the ^1H-NMR spectrum confirms the presence of an intact Ph_2PH ligand, showing the phenyl protons and a characteristic doublet [with $^1J_{PH} = 361$ Hz] for the P–H proton in a 10:1 integral ratio. A single broad resonance is seen in the $^{31}P\{^1H\}$-NMR spectrum at δ 15.4 indicative of co-ordination to cobalt (^{59}Co has a large quadrupolar moment). The $^{13}C\{^1H\}$-NMR spectrum at 293 K shows that **1** is highly fluxional, with the carbonyls appearing as a single resonance at δ 202.5 at this temperature. This observation is consistent with the results obtained previously for the complex $[Co_2Fe(\mu_3\text{-}S)(CO)_8(PBu^n_3)]$ in which a four-stage carbonyl exchange process has been identified [10].

Complex **2** again shows properties similar to those found for other disubstituted phosphine derivatives of $[Co_2Fe(\mu_3\text{-}S)(CO)_9]$ [10]. As with **1**, the ^1H-NMR spectrum shows a doublet [$^1J_{PH} = 356$ Hz] and a multiplet for the co-ordinated secondary phosphine P–H and phenyl proton resonances, respectively, and the single broad $^{31}P\{^1H\}$-NMR peak [δ 15.3] indicates that the two P atoms are equivalent and located on two different cobalt centres. The $^{13}C\{^1H\}$-NMR spectrum of **2** at 293 K as with **1**, exhibits only one carbonyl resonance, suggesting that all the carbonyl ligands are undergoing rapid exchange on the NMR timescale at room temperature.

The NMR spectrum of **3** is different from those of **1** and **2** as in this instance there are two different Ph_2PH environments. The ^1H-NMR spectrum shows two doublets [$^1J_{PH} = 343$ and 349 Hz] in a 1:2 ratio for the P–H protons, one centred at δ 6.14 (iron-bonded Ph_2PH) and the other at δ 6.04 (cobalt-bonded Ph_2PH), respec-

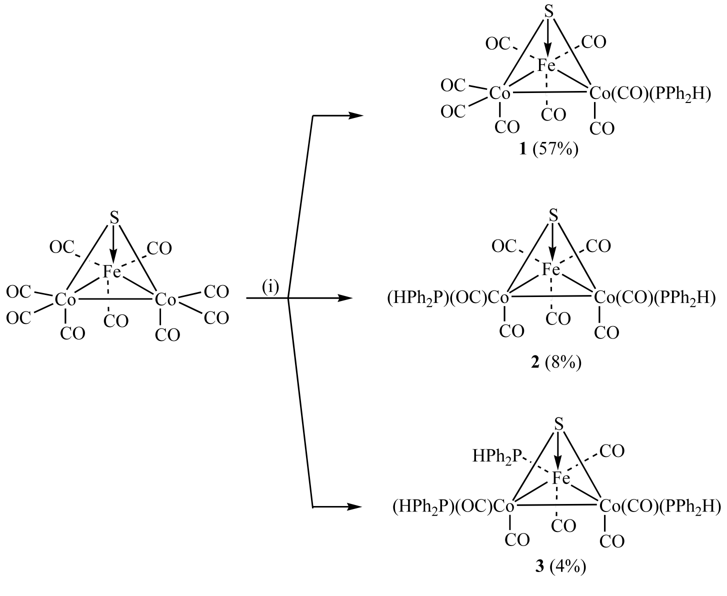

Scheme 1. Products from the reaction of $[Co_2Fe(\mu_3\text{-}S)(CO)_9]$ with diphenylphosphine in a 1:1 ratio: (i) Ph_2PH, 313 K, C_7H_8, 25 min.

Table 1
Infrared, ^{1}H- and ^{31}P-NMR data for the new complexes **1**–**8**

Compound	ν(CO) (cm^{-1}) [a]	^{1}H-NMR (δ) [b]	^{31}P-NMR (δ) [c]
1	2081m, 2033vs, 2014s, 1883w, 1959w	7.6–7.4 [m, 10H, Ph], 6.13 [d, 1H, $^{1}J_{PH}$ 361, Co-PPh$_2$*H*]	15.4 [s, Co-*P*Ph$_2$H]
2	2049s, 2009vs, 1988sh, 1943m	7.6–7.1 [m, 20H, Ph], 5.99 [d, 2H, $^{1}J_{PH}$ 356, Co-PPh$_2$*H*]	15.3 [s, Co-*P*Ph$_2$H]
3	2020s, 1978vs, 1960s, 1900w	7.7–7.1 [m, 30H, Ph], 6.14 [d, 1H, $^{1}J_{PH}$ 343, Fe-PPh$_2$*H*], 6.04 [d, 2H, $^{1}J_{PH}$ 349, Co-PPh$_2$*H*]	44.7 [s, Fe-*P*Ph$_2$H], 17.7 [s, br, Co-*P*Ph$_2$H]
4	2046m, 2005s, 1961w	7.6–7.3 [m, 20H, Ph]	226.2 [μ-*P*Ph$_2$]
5	2048w, 2017m, 1988s,1972s, 1945w	7.8–7.1 [m, 30H, Ph], 6.42 [dd, 1H, $^{1}J_{PH}$ 364, $^{3}J_{PH}$4.7, Ph$_2$P*H*]	224.8 [s, br, μ-*P*Ph$_2$], 206.2 [s, br, μ-*P*Ph$_2$], 34.4 [s, br, Co-*P*Ph$_2$H]
5′	2047s, 2019m, 1988s,1973s, 1948w	7.7–7.2 [m, 25H, Ph], 1.62 [d, 3H, $^{2}J_{PH}$ 9.5, PhP*Me*$_a$Me$_b$], 1.35 [d, 3H, ^{2}J) 9.7, PhPMe$_a$*Me*$_b$]	230.6 [s, br, μ-*P*Ph$_2$], 194.6 [s, br, μ-*P*Ph$_2$], −112.0 [s, br, Co-*P*PhMe$_2$]
6	2059w, 2039s, 2010s, 1993sh	7.9–7.3 [m, 20H, Ph]	91.0 [s, br, μ-*P*Ph$_2$], −47.7 [d, Ph$_2$*P*S, $^{2}J_{PP}$ 73]
7a	2055s, 2017vs, 2000s, 1946w	7.7–7.3 [m, 10H, Ph], 3.56 [br, 1H, CH$_2$], 3.42 [br, 1H, CH$_2$], 2.34 [s, 3H, Me]	36.9 [s, Ph$_2$*P*CH$_2$Sme]
7b	2055s, 2018vs, 1999s,1946w	7.7–7.3 [m, 15H, Ph], 3.82 [dd, $^{gem}J_{HH}$ 11.5, $^{2}J_{PH}$ 6.6, 1H, CH$_2$], 3.71 [dd, $^{2}J_{PH}$ 9.2, 1H, CH$_2$]	32.3 [s, Ph$_2$*P*CH$_2$SPh]
8	2058s, 2021vs, 2006s,1950w	7.8–7.3 [m, 10H, Ph], 2.71 [s, 3H, S*Me*]	63.9 [s, Ph$_2$*P*C(SMe)=S]

[a] Recorded in *n*-hexane solution.

[b] ^{1}H chemical shifts (δ) in ppm relative to SiMe$_4$ (0.0 ppm), coupling constants in Hz in CDCl$_3$ at 293 K.

[c] ^{31}P chemical shifts (δ) in ppm relative to 85% external H$_3$PO$_4$ (0.0 ppm) (upfield shifts negative). Spectra were {^{1}H}-gated decoupled and measured in CDCl$_3$ at 293 K.

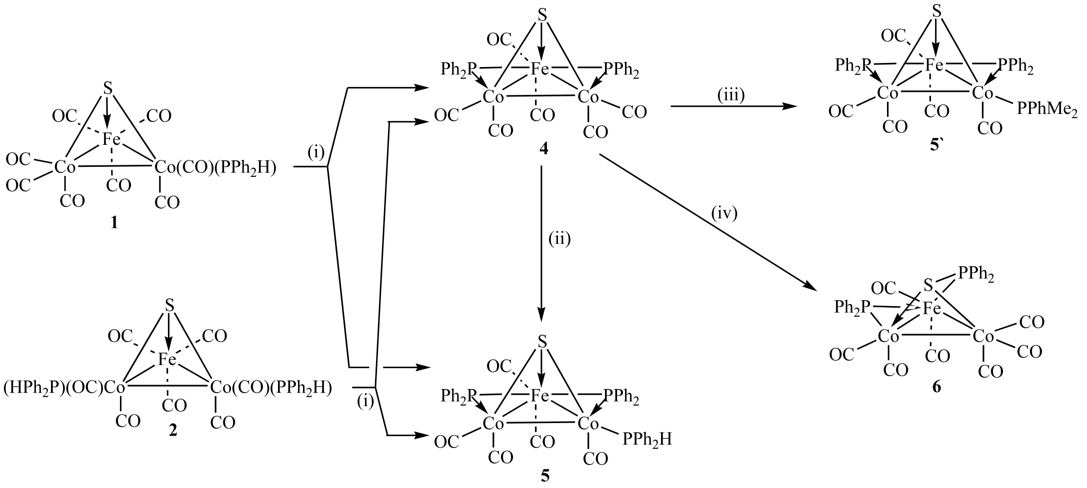

Scheme 2. Reagents and conditions: (i) 353 K, C_7H_8, 20 h; (ii) Ph_2PH, 313 K, C_7H_8, 20 h; (iii) $PhPMe_2$, 313 K, C_7H_8, 45 min; (iv) CO (70 atm.), 423 K, C_7H_8, 2 h.

tively. In the ^{31}P{^{1}H}-NMR spectrum of **3**, there is a sharp singlet at δ 44.7 corresponding to the iron-bound Ph$_2$PH, and a broad resonance at δ 17.7 corresponding to the two cobalt-bound Ph$_2$PH ligands. As with the spectra for **1** and **2**, the ^{13}C{^{1}H}-NMR spectrum of **3** shows only one carbonyl resonance at 293 K.

2.2. Thermolyses of 1 and 2

The thermolyses of [Co$_2$Fe(μ$_3$-S)(CO)$_8$(PPh$_2$H)] **1** and [Co$_2$Fe(μ$_3$-S)(CO)$_7$(PPh$_2$H)$_2$] **2** were carried out to ascertain whether P–H bond cleavage could be achieved. On heating either **1** or **2** at 353 K in toluene over 16 h green crystalline [Co$_2$Fe(μ$_3$-S)(μ-PPh$_2$)$_2$(CO)$_6$] **4** and green–brown [Co$_2$Fe(μ$_3$-S)(μ-PPh$_2$)$_2$(CO)$_5$(PPh$_2$H)] **5** were obtained in similar yields [25% **4**, 4–8% **5**] for both reactions. An improved yield of **5** was achieved by treatment of **4** with Ph$_2$PH in toluene at 313 K (82%). Similarly, the tertiary phosphine analogue of **5**, [Co$_2$Fe(μ$_3$-S)(μ-PPh$_2$)$_2$(CO)$_5$(PPhMe$_2$)] **5′**, was formed in near quantitative yield from the reaction of **4** with PhPMe$_2$ at ambient temperature (Scheme 2).

Complexes **4**, **5** and **5′** were characterised by IR, ^{1}H, ^{31}P, ^{13}C-NMR spectroscopy and by mass spectrometry and microanalysis (Table 1 and Section 3). In addition, **5′** has been the subject of a single crystal X-ray structure determination.

A partial determination of the molecular structure of complex **4** was made [13], but the poor quality of the data precludes discussion of the structural details. The X-ray analysis is, however, consistent with the proposed structure. Furthermore, the spectroscopic properties of **4** are in agreement with the solid state structure being maintained in solution. In the ^{31}P{^{1}H}-NMR spectrum, a single broad resonance is observed at δ 226.2 consistent with the two bridging phosphido groups being equivalent. The ^{13}C{^{1}H}-NMR spectrum recorded at 293 K clearly shows two triplets with $^2J_{PC} = 12.6$ and 1.7 Hz corresponding to the axial and equatorial iron-bound CO ligands (non-fluxional at room temperature). The cobalt-bound carbonyl groups appear as broad signals centred at δ 209.6 and 204.7, implying that the axial carbonyls do not exchange at room temperature with the equatorial carbonyls. This observation suggests that the presence of the two bridging phosphido groups in some way discourages any fluxional process involving exchange of carbonyls between metal centres, which might otherwise be operational at room temperature. It is noteworthy that in the complex [$Co_2Fe(\mu\text{-}PPh_2)_2(\mu\text{-}CO)(CO)_7$], which differs from **1** only in that it lacks a capping sulphur atom, all eight carbonyls can interchange readily at room temperature [14]. Clearly the capping sulphur atom plays a role in inhibiting intramolecular carbonyl exchange at room temperature. The absence of localised site exchange may be due to the bridging phosphido groups inhibiting any twist of the carbonyls at the metal centres, which has been shown to be involved in the process of exchange in dicobalt alkyne-bridged species [15].

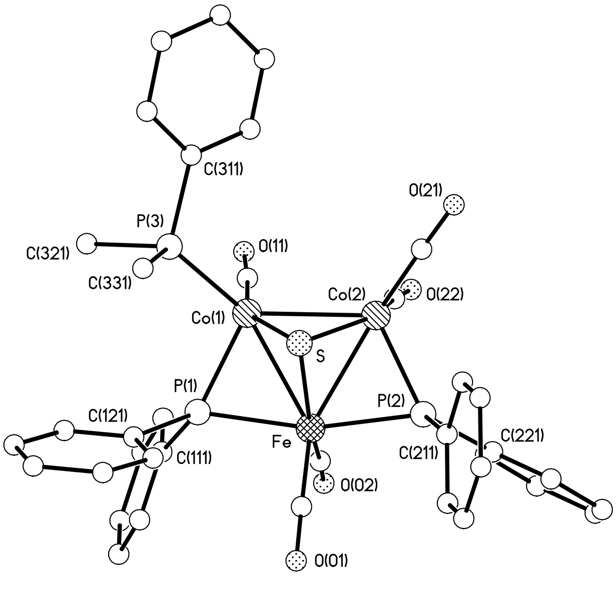

Fig. 1. Molecular structure of **5′** including the atom numbering scheme. Hydrogen atoms have been omitted for clarity.

Table 2
Selected bond lengths (Å) and angles (°) for species [$Co_2Fe(\mu_3\text{-}S)(\mu\text{-}PPh_2)_2(CO)_5(PPhMe_2)$] **5′**

Bond lengths			
Co(1)–Co(2)	2.526(1)	Co(1)–Fe	2.575(1)
Co(1)–S	2.153(2)	Co(1)–P(1)	2.155(2)
Co(1)–P(3)	2.173(2)	Co(2)–Fe	2.539(1)
Co(2)–S	2.177(2)	Co(2)–P(2)	2.178(2)
Fe–S	2.266(2)	Fe–P(1)	2.247(2)
Fe–P(2)	2.258(2)	Co(1)–C(4)	2.086(3)
C(2)–C(3)	1.454(4)	Co(1)–C(6)	1.728(3)
	C–O (carbonyl)	1.167–1.191	
Bond angles			
Fe–Co(1)–Co(2)	59.7(1)	S–Co(1)–Co(2)	54.8(1)
S–Co(1)–Fe	56.4(1)	P(1)–Co(1)–Co(2)	115.5(1)
P(1)–Co(1)–Fe	55.9(1)	P(1)–Co(1)–S	90.3(1)
P(3)–Co(1)–Co(2)	130.6(1)	P(3)–Co(1)–Fe	144.2(1)
P(3)–Co(1)–S	98.9(1)	P(3)–Co(1)–P(1)	104.1(1)
S–Co(2)–Fe	56.8(1)	P(2)–Co(2)–Co(1)	117.3(1)
P(2)–Co(2)–Fe	56.6(1)	Co(2)–Fe–Co(1)	59.2(2)
S–Fe–Co(1)	52.3(1)	S–Fe–Co(2)	53.5(1)
P(1)–Fe–Co(1)	52.6(1)	P(1)–Fe–Co(2)	111.7(1)
P(1)–Fe–S	85.1(1)	P(2)–Fe–Co(1)	112.5(1)
P(2)–Fe–Co(2)	53.6(1)	P(2)–Fe–S	81.9(1)
P(2)–Fe–P(1)	164.7(1)	Co(2)–S–Co(1)	71.4(1)
Fe–P(2)–Co(2)	69.8(1)	Fe–S–Co(2)	69.7(1)
Fe–S–Co(1)	71.2(1)	S–Co(2)–Co(1)	53.9(1)
Fe–Co(2)–Co(1)	61.1(1)	Fe–P(1)–Co(1)	71.6(1)

Suitable crystals of **5′** for X-ray diffraction (XRD) study were grown by diffusion of hexane into a dichloromethane solution of **5′** at 253 K. The structure is shown in Fig. 1, selected bond distances and angles are given in Table 2.

The molecule consists of a triangle of metal atoms, Co_2Fe, capped by a sulphur atom to give a pseudotetrahedral core. Similar cores have been identified for a number of crystallographically characterised complexes [7,12,16] including [$Co_2Fe(\mu_3\text{-}S)(CO)_9$] [16a] and [$Co_2Fe\{\mu_3\text{-}S(Cr(CO)_5)\}(CO)_9$] [16b]. In addition, each Fe–Co bond is bridged equatorially by a diphenylphosphido group with the Fe–P distances [2.247(2), 2.258(2) Å] being longer than the Co–P [2.155(2), 2.178(2) Å] distances. Two carbonyl groups complete the co-ordination spheres of Fe and Co(2), while for Co(1), a carbonyl and a $PPhMe_2$ ligand, the latter of which occupies an equatorial site. The increased steric demands imposed by the 7-coordinate iron atom may partly explain the relatively long Fe–P distances (vide supra), along with the elongated Fe–S distance [2.266(2) Å] as compared with the corresponding Co–S sulphur distances [2.153(2), 2.177(2) Å] and the average metal–sulphur distance [2.139(4) Å] in [$Co_2Fe(\mu_3\text{-}S)(CO)_9$].

The spectroscopic properties of **5′** are in accordance with the solid state structure being maintained in solution. Furthermore, on the basis of the close similarity of the spectroscopic properties of **5′**–**5**, a similar structure may be ascribed to **5** (Scheme 2). In the ^{1}H-NMR spectrum of **5**, in addition to phenyl resonances, a doublet of doublets centred at δ 6.42 with $^{1}J_{PH} = 364$ Hz and $^{3}J_{PH} = 4.7$ Hz is assigned to the P–H proton of the diphenylphosphine ligand. Complex **5′** also exhibits phenyl resonances and, in addition, shows a pair of doublets corresponding to the inequivalent methyl groups, with coupling constants $^{2}J_{PH} = 9.5$ and 9.7 Hz. In the $^{31}P\{^{1}H\}$-NMR spectrum of **5**, there are three broad singlets, two in the bridging phosphido group region [δ 224.8 and 206.2] and one signal which is further upfield [δ 34.4] and corresponds to the terminal secondary phosphine ligand. The broadness of the upfield signal provides further evidence that the phosphine is bound to a quadrupolar cobalt centre. A similar $^{31}P\{^{1}H\}$-spectrum is found for **5′** with resonances appearing at δ 230.6, 194.6 and 28.2.

While substitution of a cobalt-bound carbonyl group occurs on reaction of **4** with Ph_2PH or $PhPMe_2$ treatment of **4** with 70 atm. of CO at 423 K results in the formation of $[Co_2Fe(\mu_3\text{-}SPPh_2)(\mu\text{-}PPh_2)(CO)_7]$ **6** as the sole product in 28% yield. Although single crystals for **6** suitable for XRD could not be obtained, the spectroscopic and analytical data are consistent with the structure depicted in Scheme 2. The FAB mass spectrum displays a molecular ion peak and fragmentation peaks corresponding to the loss of up to seven carbonyl groups. In the $^{31}P\{^{1}H\}$-NMR spectrum, two resonances are observed; the downfield resonance [δ 91.0] is broad and is assigned to a phosphido group bridging an Fe–Co edge, the broadness being attributed to the presence of the quadrupolar cobalt centre. The more upfield resonance [δ -47.7] takes the form of a sharp doublet with $^{2}J_{PP} = 73$ Hz and is assigned to the Ph_2PS ligand, the sharpness of the signal supporting the co-ordination of the phosphorus centre to iron rather than cobalt. In the $^{13}C\{^{1}H\}$-NMR spectrum, in addition to aromatic resonances, four carbonyl resonances are observed at δ 209.7, 205.0, 199.8 and 198.2. The first of these is a sharp signal and is ascribed to the iron-bound carbonyls while the three more upfield resonances are broad and are assigned to the cobalt-bound carbonyls; one of these three upfield signals is due to the three carbonyls bound to the same cobalt and there are two separate resonances for the inequivalent carbonyl ligands on the other cobalt atom. We cannot entirely rule out the formulation of complex **6** as $[Co_2Fe(\mu_3\text{-}S)(\mu\text{-}PPh_2)_2(CO)_7]$, which would require the scission of an Fe–Co edge, as this also complies with the EAN rule. However, the sharpness of one of the PPh_2 signals [δ -47.7] suggests that one phosphido group is attached only to the iron atom confirming the structure shown in Scheme 2 as the more likely.

2.3. Deprotonation and reaction of **1** with electrophiles

The complex $[Co_2Fe(\mu_3\text{-}S)(CO)_8(PPh_2H)]$ **1** can be deprotonated readily using one equivalent of *n*-BuLi in THF at 195 K. The resulting anion (presumably $[Co_2Fe(\mu_3\text{-}S)(CO)_8(PPh_2Li)]$ or an oligomer based on this formula) was used for further reactions without purification. Reformation of **1** by treatment of the anion with $HBF_4{\cdot}OEt_2$ proceeded in good yield (Scheme 3).

2.3.1. Addition of $RSCH_2Cl$ ($R = Me, Ph$)

An excess of a chlorothiomethane, $RSCH_2Cl$ ($R = Me, Ph$), was added to a solution of the lithium salt of **1** and the solution stirred at 333 K for 2 h to give $[Co_2Fe(\mu_3\text{-}S)(\mu\text{-}PPh_2CH_2SR)(CO)_8]$ (R = Me **7a**, Ph **7b**), respectively, in good yield. Complexes **7a** and **7b** have been previously synthesised in similar yields by the

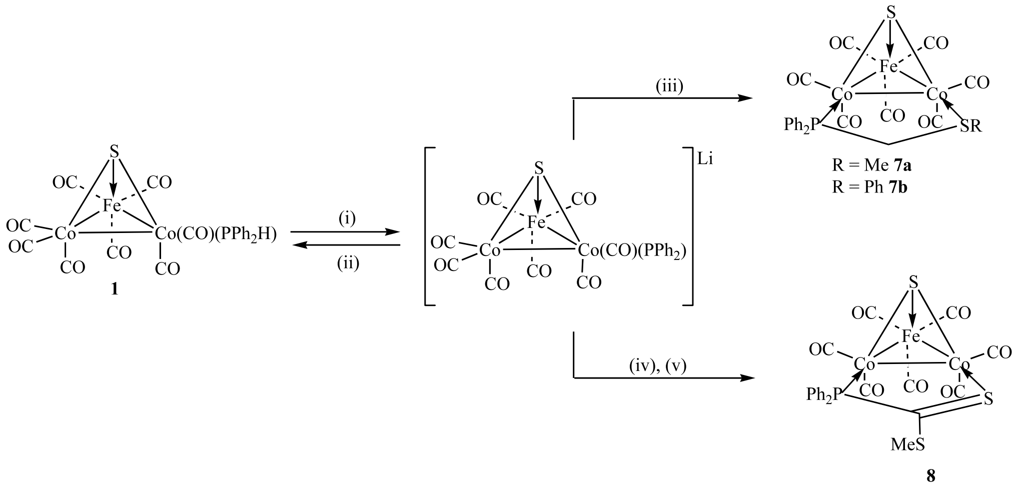

Scheme 3. Reagents and conditions: (i) *n*-BuLi, THF, 195 K; (ii) $HBF_4{\cdot}OEt_2$, THF, 293 K; (iii) $RSCH_2Cl$, THF, 333 K; (iv) xs. CS_2, THF, 293 K; (v) xs. MeI, THF, 293 K.

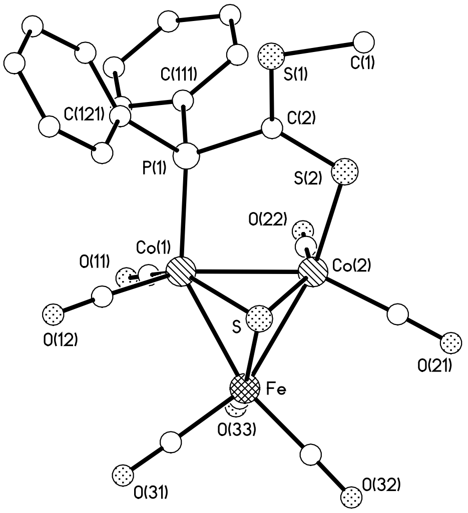

Fig. 2. Molecular structure of **8** including the atom numbering scheme. Hydrogen atoms have been omitted for clarity.

Table 3
Selected bond lengths (Å) and angles (°) for species $[Co_2Fe(\mu_3\text{-}S)\{\mu\text{-}PPh_2C(SMe){=}S\}(CO)_8]$ **8**

Bond lengths			
Co(1)–Co(2)	2.503(1)	Co(1)–Fe	2.536(2)
Co(1)–S	2.161(2)	Co(1)–P(1)	2.207(2)
Co(2)–Fe	2.536(1)	Co(2)–S	2.173(2)
Co(2)–S(2)	2.242(3)	Fe–S	2.167(3)
S(1)–C(2)	1.699(9)	S(1)–C(1)	1.790(9)
S(2)–C(2)	1.651(9)	P(1)–C(2)	1.840(7)
	C–O (carbonyl)	1.131–1.151	
Bond angles			
Fe–Co(1)–Co(2)	60.4(1)	S–Co(1)–Co(2)	55.0(1)
S–Co(1)–Fe	54.2(1)	P(1)–Co(1)–Co(2)	89.2(1)
P(1)–Co(1)–Fe	149.2(1)	P(1)–Co(1)–S	105.9(1)
Fe–Co(2)–Co(1)	60.4(1)	S–Co(2)–Co(1)	54.5(1)
S–Co(2)–Fe	54.1(1)	S(2)–Co(2)–Co(1)	100.6(1)
S(2)–Co(2)–Fe	149.2(1)	S(2)–Co(2)–S	95.3(1)
Co(2)–Fe–Co(1)	59.1(1)	S–Fe–Co(1)	54.0(1)
S–Fe–Co(2)	54.4(1)	Co(2)–S–Co(1)	70.5(1)
Fe–S–Co(1)	71.8(1)	Fe–S–Co(2)	71.5(1)
C(1)–S(1)–C(2)	103.5(5)	C(2)–S(2)–Co(2)	109.0(3)
C(2)–P(1)–Co(1)	112.8(3)	S(2)–C(2)–S(1)	124.4(4)
P(1)–C(2)–S(1)	117.4(5)	P(1)–C(2)–S(2)	118.1(5)

reaction of $[Co_2Fe(\mu_3\text{-}S)(CO)_9]$ with the pre-prepared Ph_2PCH_2SR (R = Me, Ph) ligands. The X-ray structure of **7b** reveals the Co–Co bond to be bridged equatorially by the Ph_2PCH_2SPh ligand [7].

2.3.2. Addition of CS_2 followed by MeI

An excess of carbon disulphide was added to the lithium salt of **1** and the resulting anion (presumably $[Co_2Fe(\mu_3\text{-}S)(CO)_8(PPh_2CS_2Li)]$ [17]) was methylated with methyl iodide to give $[Co_2Fe(\mu_3\text{-}S)\{\mu\text{-}PPh_2C(SMe){=}S\}(CO)_8]$ **8** in good yield. Complex **8** has been characterised spectroscopically (Table 1 and Section 3) and, in addition, has been the subject of a single crystal XRD study. Crystals of **8** suitable for an X-ray structural analysis were grown by diffusion of pentane into a dichloromethane solution of **8** at 253 K. A view of the structure of **8** is shown in Fig. 2; selected bond distances and angles are listed in Table 3.

The structure comprises a Co_2Fe triangle capped by a μ_3-S ligand with the Co–Co edge equatorially bridged by a bidentate $Ph_2PC(SMe){=}S$ ligand. The phosphorus–sulphur ligand σ-bonds to the metal centres via the phosphorus and the doubly bonded sulphur atoms and is incorporated into a twisted Co–P–C=S–Co dimetallacycle. The Co(1)–Co(2)–S(2)–C(2) unit is planar to within 0.1 Å with P(1) displaced 0.63 Å from this plane in the opposite direction to S(1). The co-ordination spheres of the metal atoms are completed by carbonyl ligands, two on each cobalt (equatorial and axial) and three on iron (two equatorial and one axial).

Within the core, the bond lengths compare closely with **7b** [7]. Both of the Co–Fe bond lengths in **8** are 2.536(2) Å which compares closely with the mean value found in **7b** [the corresponding values are 2.544(2) and 2.528(2) Å]. The Co–Co distances do differ significantly [2.503(1) Å (**8**) cf. 2.528(2) Å (**7b**)] and this is presumably due to the constraints imposed by the bridging ligand. This difference can be attributed to the fact that in **7b**, the bridging ligand contains a singly bonded P–C–S unit, whilst in **8**, the corresponding unit contains a C=S double bond. Despite the P–C–S angle being greater for **8** [118.1(5)°] as compared with **7b** [111.4(4)°] the shorter C–S bond in **8** [1.651(9) Å vs. 1.809(9) **7b**] is sufficient to shorten the Co–Co distance.

Only two crystallographically characterised complexes have been reported featuring the $Ph_2PC(SMe){=}S$ group acting as a bridging ligand [18]. Notably, in **8**, the ligand bridges in a $\eta^1(P){:}\eta^1(S)$ mode differing from the previously observed $\eta^1(P){:}\eta^1(C){:}\eta^1(S)$ mode in which the C=S bond π-bonds to one of the metal centres. Furthermore, **8** is the first example of a ligand of this type bridging metal centres linked by a metal–metal bond.

Complex **8** was also characterised by mass spectrometry (MS) and by ^1H, ^{31}P, ^{13}C-NMR and IR spectroscopy and these techniques confirm the results of the X-ray determination. In the ^1H-NMR spectrum, there is a multiplet resonance in the phenyl region and a singlet methyl group resonance (δ 2.71), whilst in the $^{31}P\{^1H\}$-NMR spectrum there is a broad singlet at δ 63.9. The $^{13}C\{^1H\}$-NMR spectrum shows a singlet for the three iron-bound carbonyls consistent with localised site exchange [10]. The Co-bound carbonyls are not clearly visible due to the quadrupolar broadening of their resonances. The central carbon of the bridging ligand is observed as a doublet at δ 132.7 with $^1J_{PC} = 52$ Hz. A doublet is also observed at δ 32.7 with $^3J_{PC} = 7$ Hz.

3. Conclusions

The co-ordinated diphenylphosphine unit in **1** has been shown to be susceptible to P–H bond cleavage, either through the use of basic conditions or by thermolysis leading to oxidative addition. Once the P–H bond has been cleaved, various further reactions can take place either involving elimination of hydrogen to give the phosphido-bridged complexes (**4**, **5**) or attack by electrophilic reagents to give the modified phosphine ligands (**7**, **8**).

4. Experimental

4.1. General techniques

All reactions were carried out under an atmosphere of dry, oxygen-free nitrogen, using standard Schlenk techniques. Solvents were distilled under nitrogen from appropriate drying agents and degassed prior to use [19]. Infrared spectra were, unless otherwise stated, recorded in hexane solution in 0.5 mm NaCl cells, using a Perkin–Elmer 1710 Fourier-transform spectrometer. Fast atom bombardment (FAB) mass spectra were recorded on a Kratos Concept instrument using 3-nitrobenzyl alcohol as a matrix. Proton (reference to $SiMe_4$), ^{31}P- and ^{13}C-NMR spectra were recorded on either a Bruker WM250 or AM400 spectrometer, ^{31}P-NMR chemical shifts are referenced to 85% H_3PO_4; all spectra were recorded in $CDCl_3$. Preparative thin-layer chromatography (TLC) was carried out on commercial Merck plates with a 0.25 mm layer of silica, or on 1 mm silica plates prepared at the University Chemical Laboratory, Cambridge. Column chromatography was performed on Kieselgel 60 (70–230 or 230–400 mesh). Products are given in order of decreasing R_f values. Elemental analyses were performed at the University Chemical Laboratory, Cambridge.

Unless otherwise stated, all reagents were obtained from commercial suppliers and used without further purification. The synthesis of $[Co_2Fe(\mu_3\text{-}S)(CO)_9]$ has been reported previously [20].

4.2. Reaction of $[Co_2Fe(\mu_3\text{-}S)(CO)_9]$ with Ph_2PH

To a solution of $[Co_2Fe(\mu_3\text{-}S)(CO)_9]$ (0.250 g, 0.55 mmol) in toluene (30 cm^3) was added a solution of Ph_2PH (0.102 g, 0.55 mmol) in toluene (10 cm^3). The solution was stirred at 313 K for 25 min. After removal of the solvent under reduced pressure, the mixture was purified using preparative TLC with hexane–dichloromethane (4:1) as eluent. This gave, in addition to a trace of the starting complex, brown crystalline $[Co_2Fe(\mu_3\text{-}S)(CO)_8(PPh_2H)]$ **1** (0.193 g, 57%), brown $[Co_2Fe(\mu_3\text{-}S)(CO)_7(PPh_2H)_2]$ **2** (0.024 g, 8%) and brown $[Co_2Fe(\mu_3\text{-}S)(CO)_6(PPh_2H)_3]$ **3** (0.021 g, 4%). **1** Anal. Found: C, 38.63; H 1.71; P 4.46. $C_{20}H_{11}O_8Co_2FePS$ Calc.: C, 38.99; H, 1.80; P 5.03%. FABMS 616 [M^+], $M^+ - n(CO)$ ($n = 1$–8). ^{13}C-NMR (^{1}H composite pulse decoupled, $CDCl_3$ at 293 K): δ 202.5 [s, 8*C*O] and 133–126 [m, Ph]. **2** Anal. Found: C, 47.73; H 2.73; P 7.93. $C_{31}H_{22}Co_2FeO_7P_2S$ Calc.: C, 48.09; H, 2.86; P 8.00%. FABMS 774 [M^+], M^+-$n(CO)$ ($n = 1$–7). ^{13}C-NMR (^{1}H composite pulse decoupled, $CDCl_3$ at 293 K): δ 209.4 [s, 7CO] and 133–128 [m, Ph]. **3** Anal. Found: C, 53.94; H 3.52; P 9.81. $C_{42}H_{33}Co_2FeO_6P_3S$ Calc.: C, 54.10; H, 3.57; P 9.97%. FABMS 932 [M^+], $M^+ - n(CO)$ ($n = 1$–6). ^{13}C-NMR (^{1}H composite pulse decoupled, $CDCl_3$ at 293 K): δ 212.6 [s, 6CO] and 134–128 [m, Ph].

*4.3. Reaction of $[Co_2Fe(\mu_3\text{-}S)(CO)_8(PPh_2H)]$ **1** with Ph_2PH*

To a solution of $[Co_2Fe(\mu_3\text{-}S)(CO)_8(PPh_2H)]$ **1** (1.0 g, 1.62 mmol) in toluene (50 cm^3) was added a solution of Ph_2PH (0.272 g, 1.46 mmol) in toluene (10 cm^3). The solution was stirred at 313 K for 3 h. After removal of the solvent under reduced pressure, the mixture was purified by flash column chromatography with hexane–dichloromethane (4:1) as eluent. This gave brown crystalline $[Co_2Fe(\mu_3\text{-}S)(CO)_7(PPh_2H)_2]$ **2** (0.988 g, 79%) and brown $[Co_2Fe(\mu_3\text{-}S)(CO)_6(PPh_2H)_3]$ **3** (0.120 g, 8%).

*4.4. Thermolysis of $[Co_2Fe(\mu_3\text{-}S)(CO)_8(PPh_2H)]$ (**1**)*

A solution of $[Co_2Fe(\mu_3\text{-}S)(CO)_8(PPh_2H)]$ **1** (0.490 g, 0.66 mmol) in THF (50 cm^3) was stirred at 353 K for a period of 17 h. After removal of solvent under reduced pressure, the residue was purified by flash chromatography with hexane–dichloromethane (9:1) as eluent. This gave some starting material, green crystalline $[Co_2Fe(\mu_3\text{-}S)(\mu\text{-}PPh_2)_2(CO)_6]$ **4** (0.122 g, 25%) and green crystalline $[Co_2Fe(\mu_3\text{-}S)(\mu\text{-}PPh_2)_2(CO)_5(PPh_2H)]$ **5** (0.034 g, 6%). **4** Anal. Found: C, 48.23; H, 2.78. $C_{30}H_{20}Co_2FeO_6P_2S$ Calc.: C, 48.42; H, 2.71%. FABMS 744 [M^+], M^+-$n(CO)$ ($n = 1$–6). ^{13}C-NMR (^{1}H composite pulse decoupled, $CDCl_3$ at 293 K): δ 213.8 [t, $^2J_{PC}$ 13, Fe*C*O], 211–208 [br, 2Co*C*O], 206.7 [t, $^2J_{PC}$ 13, Fe*C*O], 206–204 [br, 2Co*C*O] and 143–128 [m, Ph]. **5** Anal. Found: C, 54.79; H 3.70; P 10.05. $C_{41}H_{31}Co_2FeO_5P_3S$ Calc.: C, 54.57; H, 3.46; P 10.30%. FABMS 902 [M^+], M^+-$n(CO)$ ($n = 1$–5). ^{13}C-NMR (^{1}H composite pulse decoupled, $CDCl_3$ at 293 K): δ 205.4 [br, 5Co*C*O] and 134–128 [m, Ph].

*4.5. Thermolysis of $[Co_2Fe(\mu_3\text{-}S)(CO)_7(PPh_2H)_2]$ (**2**)*

A solution of $[Co_2Fe(\mu_3\text{-}S)(CO)_7(PPh_2H)_2]$ (**2**) (1.250 g, 1.61 mmol) in toluene (50 cm^3) was stirred at 353 K for 20 h. After the solvent was removed under reduced pressure, the mixture was purified by flash column chromatography with hexane–dichloromethane (9:1) as eluent. This gave brown crystalline [$Co_2Fe(\mu_3$-S)$(CO)_8(PPh_2H)$] **1** (0.277 g, 23%), green crystalline [$C_{O_2}Fe(\mu_3$-S)(μ-$PPh_2)_2(CO)_6$] **4** (0.304 g, 25%), unreacted starting material, green crystalline [$Co_2Fe(\mu_3$-S)(μ-$PPh_2)_2(CO)_5(PPh_2H)$] **5** (0.118 g, 8%) and a trace of crystalline [$Co_2Fe(\mu_3$-S)$(CO)_6(PPh_2H)_3$] **3**.

4.6. Reaction of [$Co_2Fe(\mu_3$-S)(μ-$PPh_2)_2(CO)_6$] **4** with Ph_2PH or $PhPMe_2$

4.6.1. With Ph_2PH

To a solution of [$Co_2Fe(\mu_3$-S)(μ-$PPh_2)_2(CO)_6$] **4** (0.200 g, 0.27 mmol) in toluene (30 cm^3) was added Ph_2PH (0.050 g, 0.27 mmol) and the mixture stirred at 313 K for 2 h. After the removal of solvent under reduced pressure, the residue was purified by column chromatography, eluting with hexane–dichloromethane (4:1), to yield green crystalline [$Co_2Fe(\mu_3$-S)(μ-$PPh_2)_2$-$(CO)_5(PPh_2H)$] **5** (0.199 g, 82%).

4.6.2. With $PhPMe_2$

To a solution of [$Co_2Fe(\mu_3$-S)(μ-$PPh_2)_2(CO)_6$] **4** (0.250 g, 0.34 mmol) in toluene (30 cm^3) was added $PhPMe_2$ (0.046 g, 0.34 mmol) and the mixture stirred at 293 K for 45 min. After the removal of solvent under reduced pressure, the residue was purified by column chromatography, eluting with hexane–dichloromethane (4:1), to yield green crystalline [$Co_2Fe(\mu_3$-S)(μ-$PPh_2)_2$-$(CO)_5(PPhMe_2)$] **5′** (0.244 g, 85%). **5′** FABMS 854 [M^+], $M^+ - n(CO)$ ($n = 1$–5).

4.7. Carbonylation of [$Co_2Fe(\mu_3$-S)(μ-$PPh_2)_2(CO)_6$] **4**

A solution of [$Co_2Fe(\mu_3$-S)(μ-$PPh_2)_2(CO)_6$] (**4**) (0.420 g, 0.56 mmol) in toluene (70 cm^3) was added to a Roth autoclave (100 cm^3) and pressurised with CO (70 atm). The sealed system was stirred at 423 K for 2 h. After removal of the solvent under reduced pressure, the dark red residue was redissolved in the minimum quantity of dichloromethane, adsorbed onto silica and chromatographically separated, eluting with hexane–dichloromethane (19:1) to give red [$Co_2Fe(\mu_3$-$SPPh_2)(\mu$-$PPh_2)(CO)_7$] **6** (0120 g, 28%) and a trace of starting material. **6** FABMS 772 [M^+], M^+-$n(CO)$ ($n = 1$–7). ^{13}C-NMR (^1H composite pulse decoupled, $CDCl_3$ at 293 K): δ 209.7 [s, 2Fe – *C*O], 205.0 [br, 3Co*C*O], 199.8 [br, 1Co*C*O], 198.2 [br, 1Co*C*O] and 145–128 [m, Ph].

4.8. Reaction of [$Co_2Fe(\mu_3$-S)$(CO)_8(PPh_2H)$] **1** with n-BuLi and $RSCH_2Cl$ (R = Me, Ph)

4.8.1. R = Me

To a solution of [$Co_2Fe(\mu_3$-S)$(CO)_8(PPh_2H)$] **1** (0.300 g, 0.49 mmol) in THF (40 cm^3) at 195 K was added *n*-BuLi (0.3 cm^3, 0.49 mmol) in hexane. The mixture was allowed to warm to room temperature (r.t.), after which an excess of $MeSCH_2Cl$ (0.82 cm^3, 0.98 mmol) was added. The resulting solution was stirred at 333 K for 2 h and then filtered through silica. After removal of the volatiles under reduced pressure, TLC separation with hexane–ethylacetate (5:1) gave a trace of starting material followed by green crystalline [$Co_2Fe(\mu_3$-S)(μ-$PPh_2CH_2SMe)(CO)_8$] (**7a**) (0.164 g, 52%). **7a** FABMS 648 [M^+], M^+-$n(CO)$ ($n = 1$–7). ^{13}C-NMR (^1H composite pulse decoupled, $CDCl_3$ at 293 K): δ 212.9 [s, 3Fe – *C*O], 199.5 [br, 4Co*C*O], 135–128 [m, Ph], 48.0 [d, $^1J_{PC}$ 19, $CH_2$2] and 27.7 [s, SMe].

4.8.2. R = Ph

To a solution of [$Co_2Fe(\mu_3$-S)$(CO)_8(PPh_2H)$] **1** (0.300 g, 0.49 mmol) in THF (40 cm^3) at 195 K was added *n*-BuLi (0.3 cm^3, 0.49 mmol) in hexane. The mixture was allowed to warm to r.t., after which an excess of $PhSCH_2Cl$ (0.13 cm^3, 0.98 mmol) was added. The resulting solution was stirred at 333 K for 2 h and then filtered through silica. After removal of the volatiles under reduced pressure, TLC separation with hexane–ethylacetate (5:1) gave a trace of starting material followed by green crystalline [$Co_2Fe(\mu_3$-S)(μ-PPh_2CH_2-$SPh)(CO)_8$] **7b** (0.224 g, 65%). **7b** FABMS 710 [M^+], M^+-$n(CO)$ ($n = 1$–7). ^{13}C-NMR (^1H composite pulse decoupled, $CDCl_3$ at 293 K): δ 212.8 [s, 3Fe-*C*O], 200.0 [br, 4Co*C*O], 134–128 [m, Ph] and 49.4 [d, $^1J_{PC}$ 17, $CH_2$2].

4.9. Reaction of [$Co_2Fe(\mu_3$-S)$(CO)_8(PPh_2H)$] **1** with n-BuLi, CS_2 and MeI

To a solution of [$Co_2Fe(\mu_3$-S)$(CO)_8(PPh_2H)$] **1** (0.425 g, 0.69 mmol) in THF (40 cm^3) at 195 K was added *n*-BuLi (0.4 cm^3, 0.49 mmol) in hexane. The mixture was allowed to warm to r.t., after which a 5-fold excess of CS_2 (0.262 g, 3.45 mmol) was added. The resulting solution was stirred at 293 K for 3 h, after which an excess of MeI (0.490 g, 3.35 mmol) was added. After further stirring at ambient temperature for 1 h, removal of the volatiles under reduced pressure, followed by TLC separation with hexane–dichloromethane (7:3) as eluent, gave the purple crystalline complex [$Co_2Fe(\mu_3$-S){μ-$PPh_2C(SMe)$=S}$(CO)_8$] **8** (0.252 g, 54%). **8** Anal. Found: C, 36.83; H 1.82; P 4.51. $C_{21}H_{13}Co_2FeO_7PS_3$ Calc.: C, 37.19; H, 1.93; P 4.57%. FAB MS 678 [M^+], $M^+ - n(CO)$ ($n = 1$–7). ^{13}C-NMR (^1H composite pulse decoupled, $CDCl_3$ at 293 K): δ 212.6 [s, 3Fe*C*O], 205.0

[br, Co*C*O], 134–128 [m, Ph], 132.7 [d, $^1J_{PC}$ 52, $Ph_2PC(SMe)$=S] and 32.7 [d, $^3J_{PC}$ 7, SMe].

4.10. Crystal structure determinations of complexes ***5′*** *and* ***8***

X-ray intensity data were collected with graphite-monochromated Mo–K_α radiation ($\lambda = 0.71073$ Å) radiation, on a PW1100 four-circle diffractometer at 293(2) K for **5′** and **8**. Details of data collection, refinement and crystal data are listed in Table 4. Lorentz-polarisation and absorption corrections were applied to the data of all the compounds. The positions of the metal atoms were deduced from Patterson syntheses. The remaining non-hydrogen atoms were revealed from subsequent difference-Fourier syntheses. Refinement was based on F [21].

Table 4
Crystal data and structure refinement parameters for complexes **5′** and **8**

	5′	**8**
Empirical formula	$C_{37}H_{31}Co_2FeO_5P_3S$	$C_{21}H_{13}Co_2FeO_7PS_3$
Formula weight	854.34	678.10
Crystal system	Triclinic	Triclinic
Space group	$C\bar{1}$ (alt no. 2)	$P\bar{1}$
Unit cell dimensions		
a (Å)	22.667(5)	11.060(4)
b (Å)	12.833(3)	12.365(4)
c (Å)	13.520(3)	10.924(4)
α (°)	90.41(2)	90.55(1)
β (°)	107.53(3)	95.284(1)
γ (°)	90.01(2)	115.99(1)
U (Å^3)	3724(3)	1342(1)
Z	4	2
μ(Mo–K_α) (mm^{-1})	1.52	1.68
F(000)	1736	676
Colour, habit	Black prism	Black prism
Crystal size (mm)	0.36 × 0.36 × 0.38	0.32 × 0.27 × 0.38
θ-range (°)	3.00–25.00	3.00–25.00
Limiting *hkl* indices	−24 to 24, 0–16, −15 to 15	−12 to 12, −14 to 14, 0–11
Reflections collected	6844	4981
Independent reflections	4657 [b]	2859 [b]
Data/restraints/ parameters	4657/0/191	2859/0/222
Final R indices [a]		
$[I > 2\sigma(I)]$	$R_1 = 0.0684$, $R' = 0.0747$	$R = 0.0503$, $R' = 0.0521$
All data		
Min. and max. peak/hole (e Å^{-3})	1.09 and −0.865	0.658 and −0.583

[a] $R_1 = \Sigma||F_o| - |F_c||/\Sigma|F_o|$, $wR_2 = \Sigma\,[w(F_o^2 - F_c^2)^2]/\Sigma[w(F_o^2)^2]^2$, $w^{-1} = [\sigma^2(F_o)^2 + (aP)^2 + bP]$ with $a = 0.0512$ and $b = 2.8561$ for **4**, $P = [\max(F_o^2, 0) + 2(F_c^2)]/3$.

[b] Weights of $1/\sigma^2(F)$ were applied; $[I/\sigma(I) > 3]$; $R = \Sigma(\Delta F)/\Sigma(F_o)$; $R' = [\Sigma(\Delta F)^2/\Sigma w(F_o)^2]^2$.

5. Supplementary material

Crystallographic data for the structural analysis have been deposited with the Cambridge Crystallographic Data Centre, CCDC nos. 168019–168020. Copies of this information may be obtained free of charge from: The Director, CCDC, 12 Union Road, Cambridge CB2 1EZ, UK (Fax: +44-1223-336033; e-mail: deposit@ccdc.cam.ac.ul or www: http://www.ccdc.cam.ac.uk).

Acknowledgements

This work was supported by BP Chemicals, Sunbury (to C.-Y.M.).

References

[1] (a) A.J. Carty, Adv. Chem. Ser. 196 (1982) 163;
(b) D.A. Roberts, G.L. Geoffroy, in: G. Wilkinson, F.G.A. Stone, E.W. Abel (Eds.), Comprehensive Organometallic Chemistry, Pergamon, London, 1982 Chapter 40;
(c) G. Hogarth, M.H. Lavender, J. Chem. Soc. Dalton Trans. (1992) 2759;
(d) P. Dunn, J.C. Jeffery, P. Sherwood, J. Organomet. Chem. 311 (1986) C55;
(e) M.R. Bradford, N.G. Connelly, N.C. Harrison, J.C. Jeffery, Organometallics 8 (1989) 182;
(f) J.C. Jeffery, J.G. Lawrence-Smith, J. Chem. Soc. Chem. Commun. 17 (1986);
(g) G.A. Acum, M.J. Mays, P.R. Raithby, H.R. Powell, G. A. Solan, J. Chem. Soc. Dalton Trans. (1997) 3427.

[2] (a) A.J.M. Caffyn, M.J. Mays, P. R. Raithby, J. Chem. Soc. Dalton Trans. (1992) 515;
(b) A.J.M. Caffyn, M.J. Mays, P.R. Raithby, J. Chem. Soc. Dalton Trans. (1991) 2349;
(c) A.D. Horton, M.J. Mays, P.R. Raithby, J. Chem. Soc. Dalton Trans. (1987) 1557.

[3] (a) K.M. Pietrusiewcz, M. Zablocka, Chem. Rev. 94 (1994) 1375;
(b) H.B. Kagan, M. Sasaki, in: S. Patai, Z. Rappoport (Eds.), The Chemistry of Organophosphorus Compounds, vol. 1, Wiley, New York, 1990.

[4] (a) W. Malisch, F.J. Rehmann, H. Jehle, J. Reising, J. Organomet. Chem. 570 (1998) 107;
(b) W. Malisch, F.J. Rehmann, H. Jehle, N. Reising Gunzelmann, Eur. J. Inorg. Chem. (1998) 1589.

[5] (a) J.E. Davies, M.J. Mays, P.R. Raithby, G.P. Shields, P.K. Tompkin, J. Chem. Soc. Chem. Commun. (1996) 2051;
(b) J.E. Davies, N. Feeder, M.J. Mays, P.K. Tompkin, A.D. Woods, Organometallics 19 (2000) 984.

[6] (a) J.D. King, M.J. Mays, G.E. Pateman, P.R. Raithby, M.A. Rennie, G.A. Solan, N. Choi, G. Conole, M. McPartlin, J. Chem. Soc. Dalton Trans. (1999) 4447;
(b) G. Conole, M. Kessler, M.J. Mays, G.E. Pateman, G.A. Solan, Polyhedron 17 (1998) 2993.

[7] A.J. Edwards, S.R. Mack, M.J. Mays, C.-Y. Mo, P.R. Raithby, M.-A. Rennie, J. Organomet. Chem. 519 (1996) 243.

[8] A. Martin, M.J. Mays, P.R. Raithby, G.A. Solan, J. Chem. Soc. Dalton Trans. (1993) 1789.

[9] N. Choi, G. Conole, M. Kessler, J.D. King, M.J. Mays, M. McPartlin, G.E. Pateman, G.A. Solan, J. Chem. Soc. Dalton Trans. (1999) 3941.

[10] S. Aime, L. Milone, R. Rosetti, P.L. Stanghellini, Inorg. Chim. Acta 25 (1977) 103.

[11] K. Burger, L. Korecz, G. Bor, J. Inorg. Nucl. Chem. 31 (1969) 1527.

[12] X.-L. Wang, Q.-L. Suo, Y-B. Wang, Q.W. Lu, J. Sun, Chin. J. Struct. Chem. (Jiegon Huaxue) 17 (1998) 96.

[13] Complex **4**: monoclinic, space group $P2_1/c$, $a = 18.550(4)$, $b = 23.135(5)$, $c = 15.122(3)$ Å; $\beta = 103.87(3)°$; $V = 6300(2)$ Å^3.

[14] D.A. Young, Inorg. Chem. 20 (1981) 2049.

[15] A.J.M. Caffyn, M.J. Mays, G.A. Solan, D. Braga, P. Sabatino, G. Conole, M. McPartlin, H.R. Powell, J. Chem. Soc. Daltons Trans. (1991) 3103.

[16] (a) D.L. Stevenson, C.H. Wei, L.F. Dahl, J. Am. Chem. Soc. 93 (1971) 6027;
(b) R. Richter, H. Vahrenkamp, Angew. Chem. 90 (1978) 474;
(c) A.R. Manning, L. O'Dwyer, P.A. McArdle, D. Cunningham, J. Chem. Soc. Chem. Commun. (1992) 897;
(d) A.R. Manning, A.J. Palmer, J. McAdam, B.H. Robinson, J. Simpson, Chem. Commun. (1998) 1577;
(e) A.R. Manning, L. O'Dwyer, P.A. McArdle, D. Cunningham, J. Organomet. Chem. 503 (1995) C46;
(f) A.R. Manning, L. O'Dwyer, P.A. McArdle, D. Cunningham, J. Organomet. Chem. 551 (1998) 139;
(g) Z. WanTao, G. -Shin, S. Syu-Tin, Zh. Neorg. Khim. 42 (1997) 1107.

[17] For related monoanionic complexes see Refs. [5,18].

[18] (a) K.-H. Yih, Y.-C. Lin, M.-C. Cheng, Y. Wang, J. Chem. Soc. Chem. Commun. (1993) 1380;
(b) K.-H. Yih, Y.-C. Lin, M.-C. Cheng, Y. Wang, J. Organomet. Chem. 474 (1994) C34;
(c) K.-H. Yih, Y.-C. Lin, M.-C. Cheng, Y. Wang, J. Chem. Soc. Dalton Trans. (1995) 1305.

[19] W.L.F. Armarego, D.D. Perrin, Purification of Laboratory Chemicals, 4th ed., Butterworths, London, 1996.

[20] (a) S.A. Khattab, L. Marko, G. Bor, B. Marko, J. Organomet. Chem. 1 (1964) 373;
(b) L. Marko, J. Takacs Inorg. Synth. 26 (1989) 243;
(c) H. Vahrenkamp, Inorg. Synth. 26 (1989) 351.

[21] G.M. Sheldrick, SHELX 76 Program for Crystal Structure Determination, University of Cambridge, Cambridge, 1976.